frontiers | Frontiers in Materials

TYPE Original Research
PUBLISHED 04 September 2023
DOI 10.3389/fmats.2023.1274489

OPEN ACCESS

EDITED BY
Muhan Wang,
Qingdao University of Technology, China

REVIEWED BY
Jun Ren,
Yunnan University, China
Jiawei Li,
Chinese Academy of Sciences (CAS), China

*CORRESPONDENCE
Zhitang Li,
lztpolycd@126.com

RECEIVED 08 August 2023
ACCEPTED 21 August 2023
PUBLISHED 04 September 2023

CITATION
Wang H, Li Z, Luo Q and Long W (2023), Effect of silt modification on the properties of magnesium phosphate cement.
Front. Mater. 10:1274489.
doi: 10.3389/fmats.2023.1274489

Effect of silt modification on the properties of magnesium phosphate cement

Haikuan Wang[1], Zhitang Li[2]*, Qiling Luo[3] and Wujian Long[3]

[1]State Key Laboratory of Hydraulic Engineering Simulation and Safety, Tianjin University, Tianjin, China, [2]Poly Changda Engineering Co., Ltd., Guangzhou, China, [3]Guangdong Province Key Laboratory of Durability for Marine Civil Engineering, Shenzhen University, Shenzhen, China

Magnesium phosphate cement (MPC), as a new type of cementitious material, is difficult to be popularized in practical applications due to its short setting time, high cost, and poor water resistance. Dredged silt (DS) is a kind of hazardous waste, which may cause serious damage to the ecological environment if it is not disposed of properly. The treatment of DS and its reuse in building materials is an economical and environmentally friendly treatment method, which not only realizes the recycling of DS but also avoids secondary pollution. Using the treated DS as a mineral admixture for modified MPC not only recycles the DS but also improves the properties of MPC. In this paper, the effect of DS modification on the properties of MPC was investigated by setting time test, mechanical property test, water resistance test, and RCM test, and also compared with the modification effect of common mineral admixtures, such as fly ash (FA) and metakaolin (Mk), and finally analyzed by combining with SEM pictures. With the increase of the dosage of FA, Mk, and DS, the compressive strength of the modified MPC all showed the trend of increasing and then decreasing, and the optimal dosage was 5%, 10%, and 15%, respectively. At the optimum dosage, Mk and FA could improve the resistance of MPC to chloride erosion, but DS could not. The three kinds of admixtures could prolong the setting time of MPC, with DS having the best effect, followed by FA, and Mk having the smallest effect. All three admixtures could improve the water resistance of MPC, and the effect of improvement was Mk > DS > FA. The microstructure of the specimen was denser when the dosage of DS was low, and when the dosage was too much, the hydration reaction of MPC was affected, resulting in incomplete hydration and reduced hydration products. This research has significant guiding significance for the treatment of DS and the modification of MPC.

KEYWORDS

silt, magnesium phosphate cement, fly ash, metakaolin, setting time, water resistance

Introduction

Magnesium phosphate cement (MPC) is composed of magnesium oxide, phosphate, retarding agent, and mineral admixture in specific proportions (Qiao et al., 2010; Haque and Chen, 2019). After adding water, the raw materials will undergo an acid-base reaction and hydration reaction, and then harden by physical action of coagulation (Sugama and Kukacka, 1983; Liu and Chen, 2016). Compared to common silicate cement, MPC possesses various advantages such as rapid setting and hardening speed, high early strength, good interfacial adhesion, durability, volumetric compatibility, and a simple production process (Feng et al., 2021; Yu et al., 2021; Huang et al., 2023). Hence, it is

widely used in emergency repair and reinforcement of bridges, highways, military projects (Yang et al., 2000), and the treatment of poisonous and harmful substances (Wang et al., 2021; Liu S. et al., 2023; Cao et al., 2023). However, several issues hinder the use of MPC in real engineering applications (Fang et al., 2023). First, its fast reaction speed and short solidification and hardening time limit the on-site construction duration. Second, MPC is comparatively expensive, with an average price of thousands of dollars per ton, surpassing that of silicate cement. Third, MPC exhibits poor water resistance, leading to shrinkage when exposed to long-term water environments. These factors greatly impede the widespread adoption of MPC. To address these problems, researchers have extensively studied MPC modification methods. The addition of various mineral dopants has been found to enhance the performance of MPC(Lu et al., 2023). Li Yue (Li and Chen, 2013) and Li Jiusu (Li et al., 2014) et al. found that the use of fly ash (FA) as a dopant reduced the formation of struvite by adsorbing PO_4^{3-}, leading to a prolongation of the setting time and an improvement in the flowability of MPC. This not only saved costs but also enhanced water resistance to some extent. Qin Zhaohui (Qin et al., 2020) et al. discovered that the partial replacement of MgO by metakaolin (Mk) had a positive impact on the compressive strength, tensile bond strength, and drying shrinkage of MPC mortar. Moreover, this replacement also resulted in an improvement in the freeze-thaw and water resistance of MPC.

Recently, with the implementation of large-scale water diversion and water conservancy projects, a significant amount of dredged silt (DS) has been generated (Zhang et al., 2015). DS is mainly fine-grained soil, rich in organic matter and various types of pollutants, with high water content, low strength, poor permeability, and high compressibility, accompanied by irritating odors (Chang et al., 2020). If not managed properly, the disposal of DS can not only impact river traffic but also contaminate the surrounding ecological environment, hindering sustainable development (Molino et al., 2014). Consequently, an urgent need exists to tackle the disposal problem of DS. Previous treatment methods like casting it into the sea, landfilling, incineration, composting, and blowing landfills have been phased out due to secondary pollution and high costs (Fytili and Zabaniotou, 2008; Kelessidis and Stasinakis, 2012). Nowadays, the principle of minimizing, rendering harmless, and resourcefully treating solid waste has made the harmless treatment and resourceful utilization of DS a research priority. Specifically, the treatment and reuse of DS in building materials offer an economical and environmentally friendly approach (Chakraborty et al., 2017; Chen et al., 2018). Not only does this practice enable DS recycling, but it also avoids secondary pollution.

The main chemical components of DS are SiO_2, Al_2O_3, CaO, etc .,(Lin et al., 2005). Volcanic ash has low reactivity, but it can improve its defects and enhance its reactivity through activation (Cyr et al., 2012; Naamane et al., 2016; Pavlík et al., 2016). Additionally, the presence of CaO gives DS a certain gelatinous property. The volcanic ash characteristics and gelatinous properties are two essential characteristics of supplementary gelling materials (Skibsted and Snellings, 2019). Supplementary gelling materials have great potential and practicality. In many countries, supplementary gelling materials, also known as mineral admixtures, have been widely used (Snellings et al., 2023). In concrete, the dosage can account for 20%–70% of the total gelling materials. Incorporating supplementary gelling materials not only reduces the use of cement but also provides many benefits in terms of performance (Schulze and Rickert, 2019). Based on this, if the activated DS is used as a mineral admixture for the modification of MPC, it can not only reduce the cost of MPC raw materials but also improve the performance of MPC.

Towards exploring the possibility of DS-modified MPC, this paper concentrates on the performance indexes of DS-modified MPC and also compares the modification effects with those of common mineral admixtures such as FA and Mk. Subsequently, the effect of DS-modified MPC was systematically investigated by various methods. The ability of DS-modified MPC to retard the hydration process was determined through setting time determination. Mechanical property tests were conducted to determine the optimal dosing of DS-modified MPC. Additionally, its durability was evaluated through water resistance and RCM tests. Finally, the micro-morphology of DS-modified MPC was analyzed using scanning electron microscopy (SEM).

TABLE 1 The chemical composition of refired magnesium oxide.

Composition	MgO	SiO_2	CaO	Fe_2O_3	Al_2O_3	LOI
Content (%)	90.15	4.68	3.44	0.84	0.74	1.01

Materials and methods

Raw materials

Magnesium oxide

The magnesium oxide (MgO) powder used in this test was obtained from Jinan Ludong Refractories Company Limited. It was produced by calcining magnesite at 1500°C–1600°C and then grinding it. It had a brownish-yellow color. The specific chemical composition of MgO is shown in Table 1.

Phosphates

The phosphate used in this test was analytically pure potassium dihydrogen phosphate (KH_2PO_4). It was an odorless white crystalline powder that was easily soluble in water. It was procured from Sinopharm Chemical Reagent Company Limited.

Fly ash

The fly ash used in this test was secondary and had a dark gray color. The chemical composition of fly ash is shown in Table 2.

Metakaolin

The metakaolin used in this test was brick red in color. It was produced in Henan Province. Metakaolin was based on kaolin and was dehydrated to form anhydrous aluminum silicate at the appropriate temperature. It had certain gelling properties. The specific chemical composition of metakaolin is shown in Table 3.

Dredged silt

The dredged silt (DS) used in this test underwent a series of treatments before the formal test. It was obtained from the silt at the bottom of a reservoir in Hebei Province. The treatment methods for the DS were as follows. Firstly, the wet silt was dewatered and cured

TABLE 2 The chemical composition of fly ash.

Composition	Al2O3	SiO2	Fe2O3	CaO	MgO	K2O	Na2O	LOI
Content (%)	38.2	38.5	4.47	5.85	0.973	0.96	0.902	5.68

TABLE 3 The chemical composition of metakaolin.

Composition	Al2O3	SiO2	Fe2O3	CaO	MgO	K2O	Na2O	LOI
Content (%)	52.56	42.62	0.44	0.37	0.26	0.45	0.26	0.58

FIGURE 1
Experimental equipment **(A)** 101-2EBS type electric heating blast drying oven **(B)** SM500 × 500 cement test mill **(C)** SX2-12-10 box-type resistance furnace.

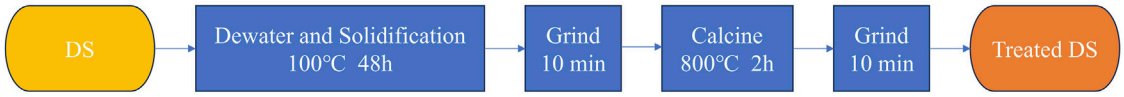

FIGURE 2
DS treatment flow diagram.

in its original state using a 101-2EBS type electric heating blast drying oven (Figure 1A). The temperature was set at 100°C and the drying time was 48 h. Next, the dewatered and solidified silt, which was in the form of large blocks, was crushed using a hammer until the maximum particle size did not exceed 45 mm. Then, the crushed silt was ground using an SM500 × 500 cement test mill (Figure 1B) for 10 min. After that, DS was calcined using an SX2-12-10 box-type resistance furnace (Figure 1C). The temperature was set at 800°C and the drying duration was 2 h. The calcined DS was then taken out and quickly cooled in the air. Finally, the slightly agglomerated DS after calcination underwent secondary ball milling for a duration of 2 min. The process flow diagram for DS treatment is shown in Figure 2. The treated DS was dark brown in color. The specific chemical composition of DS is shown in Table 4. The pre-treatment DS and post-treatment DS are shown in Figure 3.

Mixture proportions

To investigate the effect of FA, Mk, and DS on the modification of MPC, net slurry specimens with unadulterated aggregates were taken in this paper. The admixture dosage was selected as 5%, 10%, 15%, 20%, and 25%. The mass proportion of KH_2PO_4/(MgO + FA/Mk/CS) was determined as 0.4 through pre-testing. Since the particle size of the three kinds of dopants differed significantly and water consumption greatly influenced the fluidity of MPC, this test used the flow rate to control the water consumption and studied the performance of the modified MPC under the same flow rate. The test instrument used was an NLD-3 type cementitious sand flow tester, and the water consumption for a flow degree of 275 mm was selected. The specific mixture proportion is shown in Table 5.

Test methods

Setting time test

To allow sufficient operating time for MPC in engineering applications, it is necessary to study the changes in the setting time of FA, Mk, and DS doped into MPC. In this test, the setting

10.3389/fmats.2023.1274489

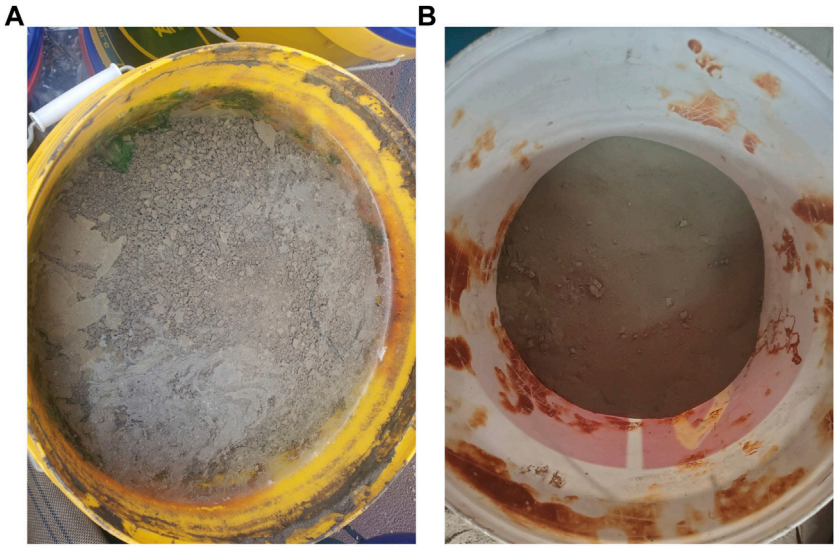

FIGURE 3
DS **(A)** pre-treatment **(B)** post-treatment.

TABLE 4 The chemical composition of dredged silt.

Composition	Al2O3	SiO2	Fe2O3	CaO	MgO	CO2	Na2O	LOI
Content (%)	16.8	55.6	8.4	8.7	3.8	6.2	0.5	5.9

TABLE 5 MPC mixture proportions of FA/Mk/DS.

MgO (%)	FA/Mk/DS	KH2PO4/(MgO + FA/Mk/DS)	Liquid-solid ratio (±0.005)
100	0	0.4	0.21
95	5%		0.22
90	10%		0.23
85	15%		0.24
80	20%		0.25
75	25%		0.26

time of modified MPC with different admixtures and different mixing ratios was measured using a Vickers meter. The measurement was conducted every 10 s during the test and every 5 s when approaching the initial setting time. Due to the short interval between the initial and final setting time of MPC, the initial setting time was considered as its setting time. The Vicat meter used in this test was produced by Wuxi Zhongke Building Material Instrument Company Limited, and the specific standards followed were GB/T2419-2005.

Mechanical property test

Compressive strength is an important indicator that characterizes the mechanical strength of cement. Compared with silicate cement, MPC is known for its fast-hardening properties, allowing it to reach a high strength within a few hours (Soudée and Péra, 2000). Therefore, the mechanical properties of modified MPC were characterized by measuring its compressive strength at 1 day, 3 days, 7 days, and 28 days. The testing instrument used was a YAW-300C automatic pressure tester. The specimens had dimensions of 30 mm × 30 mm × 30 mm, and the average compressive strength was calculated from 6 specimens. The specific standards used for this test were GB/T 17,671-2021.

Water resistance test

Water resistance refers to the ability of a material to resist external water damage and erosion, as well as the ability of a material to maintain stability and development of its properties

in an aqueous environment. For general materials, water resistance is expressed by the softening coefficient, and it is usually considered that materials with a softening coefficient greater than 0.85 are water-resistant materials. For MPC, there are many evaluation indexes for water resistance, such as mass loss rate, volume change rate, retention rate of potassium magnesium phosphate, and decay rate of potassium magnesium phosphate. These indexes mainly focus on the change of mechanical properties, which typically exhibit a decrease in water environments. In this test, the strength retention rate was used as the evaluation index for the water resistance of MPC, which is defined as follows (Liu J. et al., 2023):

$$\alpha_{\omega} = \frac{f_{d\omega}}{F_d} \tag{1}$$

where, α_{ω} is the strength retention rate of the material; $f_{d\omega}$ is the compressive strength of the material in water at the corresponding age (MPa); F_d is the compressive strength of the specimen maintained at room temperature at the corresponding age (MPa).

The test specimens were subjected to the same conditions as those maintained at room temperature, except for the maintenance method. The underwater specimen maintenance mode: after demolding, the specimen was placed in room temperature water maintenance to 28 days, followed by vacuum drying for 24 h. The dry specimen was then used for the compressive strength test, and the measured data were used to calculate the strength retention rate. The testing instrument employed was the YAW-300C automatic pressure testing machine.

Rapid chloride migration test (RCM test)

With increasing research on the water resistance of MPC and the development of preventive mechanisms for the strength inversion of MPC in water environments, there is significant potential for the application of MPC in marine construction. Given that MPC is often used as a repair material in marine engineering (Jianming et al., 2018), its resistance to chloride ion erosion needs to be investigated. RCM test is a method that reacts to the resistance of concrete to chloride ion penetration by determining the depth of penetration of chloride ions in the concrete and calculating the chloride ion mobility coefficient. The RCM test can determine the resistance of MPC-based materials to chloride ion attack before and after modification. The specimens used in this test were MPC, $MPC_{10\%FA}$, $MPC_{5\%Mk}$, and $MPC_{15\%DS}$, cured at room temperature for 28 days. The testing device utilized was an RCM-NTB type chloride ion diffusion coefficient tester from Beijing Naird Company. The chloride diffusion coefficient was calculated as follows:

$$D_{RCM} = 2.872 \times 10^{-6} \frac{Th\left(X_d - \alpha\sqrt{X_d}\right)}{t} \tag{2}$$

$$\alpha = 3.338 \times 10^{-3} \sqrt{Th} \tag{3}$$

where, D_{RCM} denotes the diffusion coefficient of chloride ions in concrete determined by the RCM method; T denotes the reaction temperature K); h denotes the height of the circular mold specimen m); X_d denotes the diffusion depth of chloride ions m); t denotes the energization time s); α is an auxiliary variable.

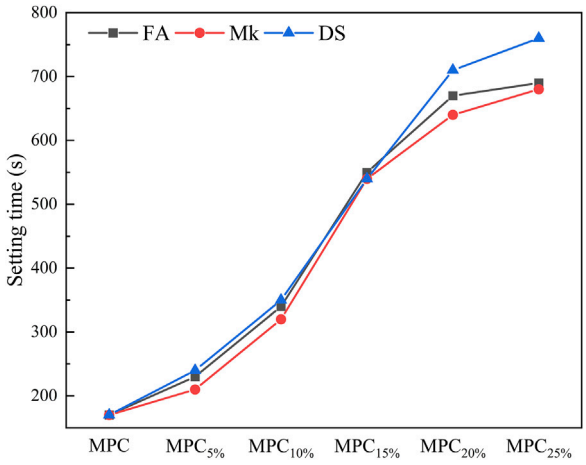

FIGURE 4
Setting time of FA/Mk/DS-modified magnesium phosphate cement.

Scanning electron microscope test (SEM test)

In this test, SEM was used to observe the microscopic morphology of DS-modified MPC with various doping amounts. After the compressive test, the specimens were crushed and the broken pieces at the center were selected as samples. These samples were submerged in isopropyl alcohol to stop hydration and then removed after 24 h for drying and grinding. The TESCAN VEA3 scanning electron microscope was used as the testing instrument for microscopic observation.

Results and discussion

Setting time

The setting times of the modified MPC are shown in Figure 4. Overall, the setting time of the modified MPC was prolonged with the increase of doping amount, indicating that all three dopants can retard the MPC reaction rate and prolong the setting time. When the dosage was the same, DS-modified MPC had the longest setting time, followed by FA, and Mk had the shortest. There are two main reasons for the prolongation of condensation time in MPC. The first reason is the decrease in reactant activity. DS has the lowest reactive aluminum content and low reactivity compared to FA and Mk, leading to prolonged condensation time (Xu et al., 2017). The second reason is that the dopant wraps around the MgO, reducing the contact surface between reactants. As the dopant dosage increases, it fails to react completely and exhibits a wrapping effect on MgO, resulting in a reduction in reaction rate and prolongation of the coagulation time.

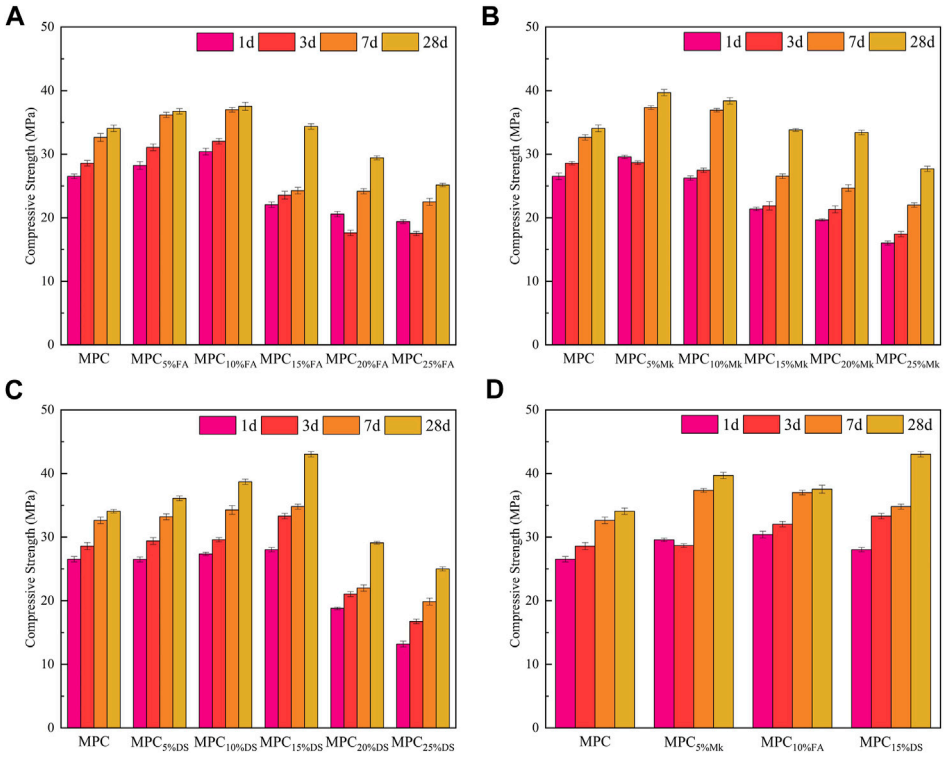

FIGURE 5
Compressive strength **(A)** MPC_{FA} **(B)** MPC_{Mk} **(C)** MPC_{DS} **(D)** comparison chart.

Mechanical property

The compressive strength values of the three mineral admixture-modified MPC for 1 day, 3 days, 7 days, and 28 days were tested using pure MPC specimens as a control group. The results are shown in Figure 5. As shown in Figure 5A when the dopant was FA, the compressive strength of modified MPC first increased and then decreased with the increase of doping. At 10% doping, the compressive strength at all ages was greater than the compressive strength at the age corresponding to the rest of the doping, reaching 37.53 MPa at 28 days, which was considered the optimal doping of FA. Compared with MPC, the compressive strength at 1 day, 3 days, 7 days, and 28 days increased by 14.6%, 12.1%, 13.4%, and 10.2%, respectively, at the optimal dosage. The increase in compressive strength when the FA dosage is less than 10% may be due to the active effect and micro aggregate effect of FA. There is a large amount of reactive SiO_2 and Al_2O_3 in FA, of which Al_2O_3 may participate in the acid-base reaction of MPC and react with PO_4^{3-} ions to produce $AlPO_4$ gelling materials. These gelling materials, together with struvite (the main hydration product of MPC, $MgNH_4PO_4{\cdot}6H_2O$), play a reinforcing role in the structure. Owing to the micro aggregate effect, the fine particles in FA can significantly improve and increase the structural strength (Ahmad et al., 2019). In addition to this, FA particles can act as nuclei in MPC, promoting the production and crystallization of struvite (Liu et al., 2022). However, the compressive strength decreases when FA doping is greater than 10%, which may be caused by the decrease in struvite due to low MgO content.

Similarly, in Figure 5B, it is observed that the compressive strength of modified MPC increased and then decreased with the increase of dosage when the dopant was Mk. The optimal dosage of Mk was 5%, and the maximum strength of 39.9 MPa was reached at 28 days. The optimal dosage increased the compressive strength of the MPC by 11.5%, 0.4%,14.4%, and 16.5% at 1 day, 3 days, 7 days, and 28 days, respectively, as compared to MPC. The reason for this improvement is that Mk is highly reactive and contains a large amount of amorphous SiO_2 and Al_2O_3, of which Al_2O_3 reacts with PO_4^{3-} ions to generate $AlPO_4$ gelling materials, which improves the MPC compressive strength (Lu and Chen, 2016). In addition, the small particle size of Mk can act as a pore filler in the MPC matrix, thereby increasing the compressive strength (Al Menhosh et al., 2016). However, the decrease in compressive strength of Mk-modified MPC is mainly due to two reasons. One is that the excess of Mk leads to the insufficient content of MgO, resulting in a reduction of struvite. Another is that Mk itself has a lamellar structure, and excessive content adversely affects the compressive strength.

Moving on to Figure 5C, it can be observed that the compressive strength of modified MPC also increased and then decreased with the increase of dosage when the dopant was DS. The optimal dosage of DS was 15%, and the maximum strength of 43.03 MPa was reached at 28 days. The optimal dosage increased the compressive strength of the modified MPC compared to the MPC compressive strengths of 5.7%, 16.5%, 6.6%, and 26.3% at 1 day, 3 days, 7 days, and 28 days. The main components of DS are SiO_2 and Al_2O_3, in which the active aluminum can be stimulated to react with

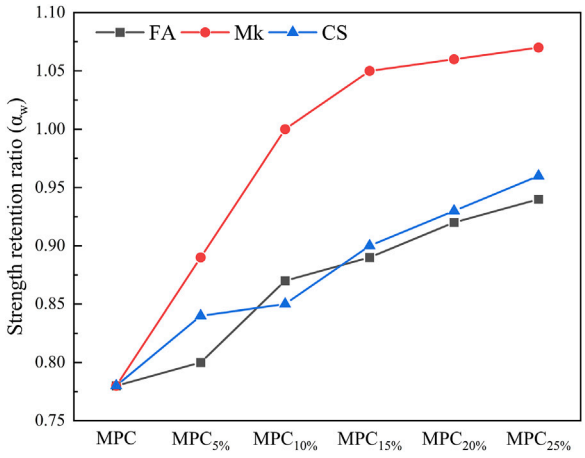

FIGURE 6
Comparison Chart 0f 28 days strength retention rate of MPC_{FA}/MPC_{Mk}/MPC_{DS}.

phosphate to generate a gelling material of aluminum phosphate salt, which in turn improves the compressive strength of MPC. Meanwhile, the filling effect of DS particles can also improve the pore structure, thus enhancing the compressive strength. However, when the DS doping exceeds 15%, the compressive strength is reduced because DS replaces MgO too much to affect the hydration reaction of MPC, leading to a decrease in the generation of hydration products, which then affects the mechanical properties.

Lastly, in Figure 5D, it is evident that the mechanical properties of 15% doped DS were the most optimal at the age of 28 days. The increased strength of modified MPC is mainly due to the filling effect of the dopant and the gelling materials generated by the active aluminum component in it being further stimulated to react. On the other hand, the decrease in strength is mainly attributed to the hydration of MPC being influenced by the excess of dopant. It is worth noting that the compressive strength of DS-modified MPC is higher due to the larger proportion of small-size DS particles, which have a better filling effect on the matrix.

Water resistance

MPC specimens were used as a control group to test the strength retention of the three mineral admixture-modified MPC at different dosages. The results are shown in Figure 6. It can be observed that the strength retention rate of MPC after 28 days of curing in water was 0.78, indicating poor water resistance. This can be attributed to the dissolution of unreacted phosphate and MgO in the matrix, resulting in increased porosity (Le Rouzic et al., 2017). Additionally, the dissolution of phosphate lowers the pH value of the solution, leading to the decomposition of struvite and a looser pore structure (Bhuiyan et al., 2007). Furthermore, white crystalline substances, identified as $MgKPO_4$, were observed on the surface of the dried matrix after conditioning in water, confirming the dissolution of struvite.

After 28 days of curing in water, the strength retention of all three modified MPC increased, indicating a gradual improvement in water resistance, corroborating previous research (Zheng et al., 2016). The incorporation of the three dopants contributed to this enhanced water resistance by generating hydration products that block capillary pore channels and alter the pore structure of the system. The active components of the dopants, Al_2O_3 and SiO_2, respectively participate in reactions to form aluminum-containing gelling materials and $MgSiO_3$(Lv et al., 2019). These reactions reduce the concentration of soluble Mg^{2+} ions and hinder water flow, leading to improved impermeability. Moreover, the dopants act as ultrafine fillers, filling the pores within the matrix, thereby increasing densification and strengthening the MPC(Li and Feng, 2011). A comparison of the three dopants revealed that MPC modified with Mk exhibited the best water resistance, followed by DS, while FA was the least effective. Notably, large amounts of Mk doping resulted in a strength retention rate greater than 1, but this corresponded to relatively low compressive strength, making it less advantageous for practical applications. Therefore, $MPC_{10\%FA}$, $MPC_{10\%Mk}$, and $MPC_{15\%DS}$ displayed better water resistance and higher compressive strength values, suggesting their suitability for prioritization in practical applications.

RCM test

Using MPC as a control, this test compared the chlorine ion erosion resistance of the three dopants at the optimum dosage. Table 6 illustrates the chloride ion diffusion coefficients of the modified MPC materials. According to Table 6, the diffusion coefficient of MPC was 7.15×10^{-12} m^2/s, which indicated its weak resistance against chloride ion erosion. In contrast, the diffusion coefficients of $MPC_{10\%FA}$ and $MPC_{5\%Mk}$ decreased by 19.19% and 21.06% respectively, compared to that of MPC. Conversely, the diffusion coefficient of $MPC_{15\%DS}$ increased by 21.2%. Thus, the incorporation of FA and Mk enhanced the resistance to chloride erosion in MPC-based materials, while DS did not. The inclusion of FA and Mk decreased the reaction rate, allowing for more thorough hydration and resulting in hydrated products with fewer crystal defects and a more stable structure. Moreover, the reactive Al_2O_3 in FA and Mk participated in the reaction, forming aluminum-containing gelling materials. These materials, along with some unreacted FA and Mk, filled the matrix pores and improved matrix densification. However, the increase in diffusion coefficient for DS may be attributed to the poor activity of DS particles and the greater intrusion of chloride ions into DS.

SEM test

The MPC specimens were used as the control group, and SEM was used to observe the microscopic morphology of MPC modified with different doping amounts of DS. The results are shown in Figures 7–9. The main hydration product of MPC is struvite ($MgKPO_4{\cdot}6H_2O$), which comprises large crystals, plate crystals, lamellar crystals, and columnar crystals (Chau et al., 2011).

Figure 7 shows the microstructure of MPC maintained for 3 days. Upon magnification of 500 times, a spatial network

TABLE 6 Chloride diffusion coefficient of modified MPC-based materials.

Specimen number	Specimen height (mm)	Color rendering depth (mm)	Diffusion coefficient ($\times 10^{-12}$ m^2/s)
MPC	50.2	16	7.150
$MPC_{10\%FA}$	50.1	13	5.778
$MPC_{5\%Mk}$	50.1	12	5.644
$MPC_{15\%DS}$	50.2	19	8.668

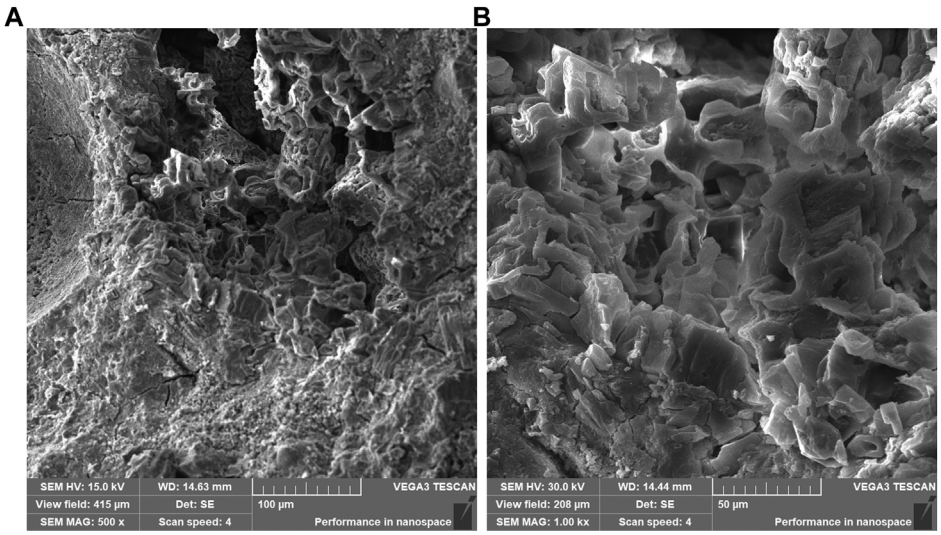

FIGURE 7
SEM images of MPC 3 days **(A)** 3 days × 500 times **(B)** 3 days × 1000 times.

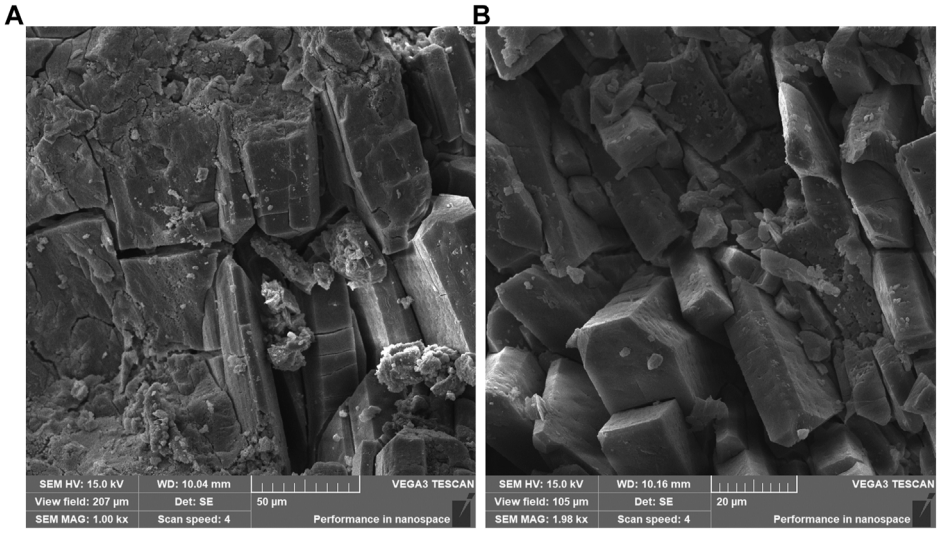

FIGURE 8
SEM images of $MPC_{15\%DS}$ 3 days **(A)** 3 days × 1000 times **(B)** 3 days × 1980 times.

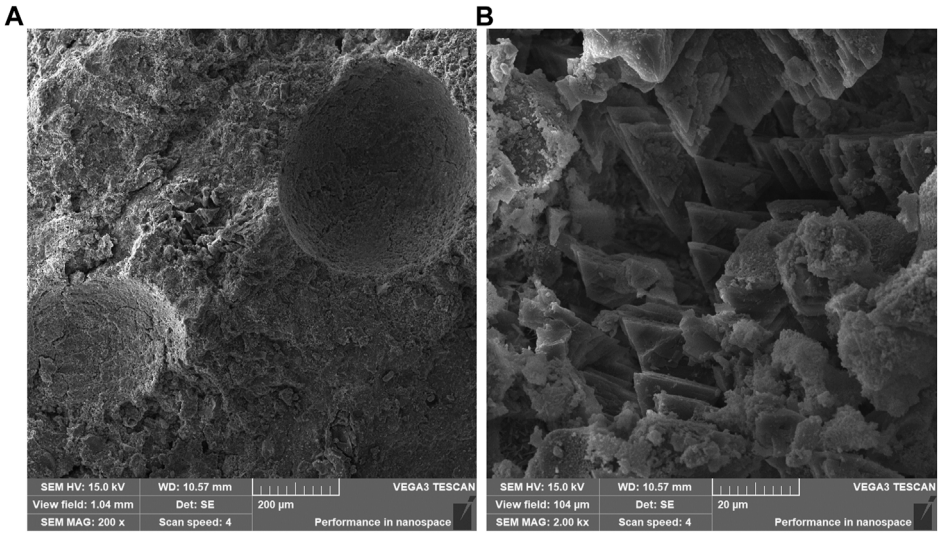

FIGURE 9
SEM images of $MPC_{25\%DS}$ 3 days **(A)** 3 days × 200 times **(B)** 3 days × 2000 times.

structure with MgO as the skeleton and struvite as the bonding phase was observed. The structure appears complete at this level of magnification. However, at a magnification of 1000 times, the main hydration product of MPC was mainly composed of columnar and layered crystals, suggesting a high degree of crystal crystallization but a relatively loose structure. Notably, the presence of large pores between the crystals is observed, indicating variations in the structure. Figure 8 presents the microstructure of $MPC_{15\%DS}$ maintained for 3 days. In this case, columnar and lamellar crystals were evident throughout the specimen, demonstrating complete and tightly arranged crystals. This suggested that the hydration of MPC was more comprehensive, leading to enhanced mechanical properties. Figure 9 illustrates the microstructure of $MPC_{25\%DS}$ maintained for 3 days. Similar to the previous case, columnar and lamellar crystals were present. However, the crystal structure defects were more pronounced, with a noticeable accumulation of cracks and holes on the surface. This indicated that the excess DS negatively affected the hydration process of MPC, resulting in incomplete hydration and reduced hydration products. Moreover, the excess DS appeared to be stacked on the crystal surface, leading to a decrease in crystallinity. These factors likely contributed to the decrease in mechanical properties observed in this scenario.

Conclusion

The effect of DS modification on the properties of MPC was investigated by comparing it with common mineral admixtures such as FA and Mk. The investigation involved setting time determination, mechanical property test, water resistance test, and RCM test. The results were analyzed by combining them with SEM pictures. The conclusions drawn are as follows.

1. The setting time of modified MPC is prolonged with the increase of doping amount. This indicates that all three dopants can retard the MPC reaction rate and extend the setting time. Among the dopants, DS-modified MPC has the longest setting time, followed by FA, and Mk has the shortest setting time when the dosage is the same.
2. The compressive strength of modified MPC shows a trend of increasing and then decreasing with the increase of the dopant dosage. The optimal dosage for the three mineral dopants, FA, Mk, and DS, are determined to be 10%, 5%, and 15% respectively. At optimal doping levels, Mk and FA improve the resistance of MPC to chloride erosion, while DS can not.
3. The incorporation of the three kinds of mineral admixtures can improve the water resistance of MPC. The modification effect in the order of Mk > DS > FA. Considering the mechanical properties, MPC doped with 10% FA, MPC doped with 10% Mk, and MPC doped with 15% DS is more suitable for practical engineering applications.
4. According to SEM analysis, when the DS doping is low, columnar and layered crystals throughout the specimen, and the addition of DS made the structure denser. However, when the DS doping is too high, these columnar and layered crystals indicate the presence of numerous stacked cracks and pores. Excessive DS affects the hydration of MPC, leading to incomplete hydration and a reduction in hydration products.

Using DS as a modification agent for MPC is an economical and environmentally friendly treatment method. This method facilitates the recycling of DS and avoids secondary pollution, while also addressing practical challenges in MPC application. It extends the operation time, reduces costs, and improves water resistance. However, it is worth noting that DS-modified MPC is less resistant to chloride erosion compared to common dopants

like FA and Mk. Further in-depth studies are needed to explore this aspect.

Data availability statement

The raw data supporting the conclusion of this article will be made available by the authors, without undue reservation.

Author contributions

HW: Data curation, Investigation, Writing–original draft. ZL: Methodology, Writing–review and editing. QL: Resources, Supervision, Validation, Writing–review and editing. WL: Project administration, Validation, Writing–review and editing.

Funding

The author(s) declare financial support was received for the research, authorship, and/or publication of this article. Financial support from the National Natural Science Foundation of China under the grant of U2006223 is gratefully acknowledged.

Conflict of interest

Author ZL was employed by the company Poly Changda Engineering Co., Ltd.

The remaining authors declare that the research was conducted in the absence of any commercial or financial relationships that could be construed as a potential conflict of interest.

Publisher's note

All claims expressed in this article are solely those of the authors and do not necessarily represent those of their affiliated organizations, or those of the publisher, the editors and the reviewers. Any product that may be evaluated in this article, or claim that may be made by its manufacturer, is not guaranteed or endorsed by the publisher.

References

Ahmad, M. R., Chen, B., and Yu, J. (2019). A comprehensive study of basalt fiber reinforced magnesium phosphate cement incorporating ultrafine fly ash. *Compos. Part B Eng.* 168, 204–217. doi:10.1016/j.compositesb.2018.12.065

Al Menhosh, A., Wang, Y., and Wang, Y. (2016). The mechanical properties of the concrete using metakaolin additive and polymer admixture. *J. Eng.* 2016, 1–6. doi:10.1155/2016/1670615

Bhuiyan, M. I., Mavinic, D. S., and Beckie, R. D. (2007). A solubility and thermodynamic study of struvite. *Environ. Technol.* 28 (9), 1015–1026. doi:10.1080/09593332808618857

Cao, X., Zhang, Q., Yang, W., Fang, L., Liu, S., Ma, R., et al. (2023). Lead-chlorine synergistic immobilization mechanism in municipal solid waste incineration fly ash (MSWIFA)-based magnesium potassium phosphate cement. *J. Hazard Mater* 442, 130038. doi:10.1016/j.jhazmat.2022.130038

Chakraborty, S., Jo, B. W., Jo, J. H., and Baloch, Z. (2017). Effectiveness of sewage sludge ash combined with waste pozzolanic minerals in developing sustainable construction material: an alternative approach for waste management. *J. Clean. Prod.* 153, 253–263. doi:10.1016/j.jclepro.2017.03.059

Chang, Z., Long, G., Zhou, J. L., and Ma, C. (2020). Valorization of sewage sludge in the fabrication of construction and building materials: A review. *Resour. Conservation Recycl.* 154, 104606. doi:10.1016/j.resconrec.2019.104606

Chau, C. K., Qiao, F., and Li, Z. (2011). Microstructure of magnesium potassium phosphate cement. *Constr. Build. Mater.* 25 (6), 2911–2917. doi:10.1016/j.conbuildmat.2010.12.035

Chen, Z., Li, J. S., and Poon, C. S. (2018). Combined use of sewage sludge ash and recycled glass cullet for the production of concrete blocks. *J. Clean. Prod.* 171, 1447–1459. doi:10.1016/j.jclepro.2017.10.140

Cyr, M., Idir, R., and Escadeillas, G. (2012). Use of metakaolin to stabilize sewage sludge ash and municipal solid waste incineration fly ash in cement-based materials. *J. Hazard Mater* 243, 193–203. doi:10.1016/j.jhazmat.2012.10.019

Fang, B., Hu, Z., Shi, T., Liu, Y., Wang, X., Yang, D., et al. (2023). Research progress on the properties and applications of magnesium phosphate cement. *Ceram. Int.* 49 (3), 4001–4016. doi:10.1016/j.ceramint.2022.11.078

Feng, H., Zhao, X., Li, L., Zhao, X., and Gao, D. (2021). Water stability of bonding properties between nano-Fe2O3-modified magnesium-phosphate-cement mortar and steel fibre. *Constr. Build. Mater.* 291, 123316. doi:10.1016/j.conbuildmat.2021.123316

Fytili, D., and Zabaniotou, A. (2008). Utilization of sewage sludge in EU application of old and new methods—a review. *Renew. Sustain. Energy Rev.* 12 (1), 116–140. doi:10.1016/j.rser.2006.05.014

Haque, M. A., and Chen, B. (2019). Research progresses on magnesium phosphate cement: A review. *Constr. Build. Mater.* 211, 885–898. doi:10.1016/j.conbuildmat.2019.03.304

Huang, X., Liu, G., Zheng, Y., and Luo, H. (2023). The performance of magnesium phosphate cement in negative temperature environment: A state-of-the-art review. *J. Build. Eng.* 76, 107278. doi:10.1016/j.jobe.2023.107278

Jianming, Y., jie, Z., and Shucong, Z. (2018). Experimental research on seawater erosion resistance of magnesium potassium phosphate cement pastes. *Constr. Build. Mater.* 183, 534–543. doi:10.1016/j.conbuildmat.2018.06.136

Kelessidis, A., and Stasinakis, A. S. (2012). Comparative study of the methods used for treatment and final disposal of sewage sludge in European countries. *Waste Manag.* 32 (6), 1186–1195. doi:10.1016/j.wasman.2012.01.012

Le Rouzic, M., Chaussadent, T., Stefan, L., and Saillio, M. (2017). On the influence of Mg/P ratio on the properties and durability of magnesium potassium phosphate cement pastes. *Cem. Concr. Res.* 96, 27–41. doi:10.1016/j.cemconres.2017.02.033

Li, D. X., and Feng, C. H. (2011). Study on modification of the magnesium phosphate cement-based material by fly ash. *Adv. Mater. Res.* 150-151, 1655–1661. doi:10.4028/www.scientific.net/amr.150-151.1655PTS 1 AND 2

Li, J., Zhang, W., and Cao, Y. (2014). Laboratory evaluation of magnesium phosphate cement paste and mortar for rapid repair of cement concrete pavement. *Constr. Build. Mater.* 58, 122–128. doi:10.1016/j.conbuildmat.2014.02.015

Li, Y., and Chen, B. (2013). Factors that affect the properties of magnesium phosphate cement. *Constr. Build. Mater.* 47, 977–983. doi:10.1016/j.conbuildmat.2013.05.103

Lin, K. L., Chiang, K. Y., and Lin, C. Y. (2005). Hydration characteristics of waste sludge ash that is reused in eco-cement clinkers. *Cem. Concr. Res.* 35 (6), 1074–1081. doi:10.1016/j.cemconres.2004.11.014

Liu, J., Yan, Y., Li, Z., Yang, F., Hai, R., and Yuan, M. (2023a). Investigation on the potassium magnesium phosphate cement modified by pretreated red mud: basic properties, water resistance and hydration heat. *Constr. Build. Mater.* 368, 130456. doi:10.1016/j.conbuildmat.2023.130456

Liu, N., and Chen, B. (2016). Experimental research on magnesium phosphate cements containing alumina. *Constr. Build. Mater.* 121, 354–360. doi:10.1016/j.conbuildmat.2016.06.010

Liu, S., Cao, X., Yang, W., Liu, R., Fang, L., Ma, R., et al. (2023b). Preparation of magnesium potassium phosphate cement from municipal solid waste incineration fly ash and lead slag co-blended: ca-Induced crystal reconstruction process and Pb-Cl synergistic solidification mechanism. *J. Hazard Mater* 457, 131690. doi:10.1016/j.jhazmat.2023.131690

Liu, Y., Chen, B., Dong, B., Wang, Y., and Xing, F. (2022). Influence mechanisms of fly ash in magnesium ammonium phosphate cement. *Constr. Build. Mater.* 314, 125581. doi:10.1016/j.conbuildmat.2021.125581

Lu, J., Wang, Q., Su, T., Yao, N., Qu, W., Cui, L., et al. (2023). PD-1 inhibitors plus chemotherapy as first-line therapy for stage IV ESCC. *J. Sustain. Cement-Based Mater.*, 1–6. doi:10.1080/1120009X.2023.2247206

Lu, X., and Chen, B. (2016). Experimental study of magnesium phosphate cements modified by metakaolin. *Constr. Build. Mater.* 123, 719–726. doi:10.1016/j.conbuildmat.2016.07.092

Lv, L., Huang, P., Mo, L., Deng, M., Qian, J., and Wang, A. (2019). Properties of magnesium potassium phosphate cement pastes exposed to water curing: A comparison study on the influences of fly ash and metakaolin. *Constr. Build. Mater.* 203, 589–600. doi:10.1016/j.conbuildmat.2019.01.134

Molino, B., De Vincenzo, A., Ferone, C., Messina, F., Colangelo, F., and Cioffi, R. (2014). Recycling of clay sediments for geopolymer binder production. A new perspective for reservoir management in the framework of Italian legislation: the occhito reservoir case study. *Mater. (Basel)* 7 (8), 5603–5616. doi:10.3390/ma7085603

Naamane, S., Rais, Z., and Taleb, M. (2016). The effectiveness of the incineration of sewage sludge on the evolution of physicochemical and mechanical properties of Portland cement. *Constr. Build. Mater.* 112, 783–789. doi:10.1016/j.conbuildmat.2016.02.121

Pavlík, Z., Fořt, J., Záleská, M., Pavlíková, M., Trník, A., Medved, I., et al. (2016). Energy-efficient thermal treatment of sewage sludge for its application in blended cements. *J. Clean. Prod.* 112, 409–419. doi:10.1016/j.jclepro.2015.09.072

Qiao, F., Chau, C. K., and Li, Z. (2010). Property evaluation of magnesium phosphate cement mortar as patch repair material. *Constr. Build. Mater.* 24 (5), 695–700. doi:10.1016/j.conbuildmat.2009.10.039

Qin, Z., Ma, C., Zheng, Z., Long, G., and Chen, B. (2020). Effects of metakaolin on properties and microstructure of magnesium phosphate cement. *Constr. Build. Mater.* 234, 117353. doi:10.1016/j.conbuildmat.2019.117353

Schulze, S. E., and Rickert, J. (2019). Suitability of natural calcined clays as supplementary cementitious material. *Cem. Concr. Compos.* 95, 92–97. doi:10.1016/j.cemconcomp.2018.07.006

Skibsted, J., and Snellings, R. (2019). Reactivity of supplementary cementitious materials (SCMs) in cement blends. *Cem. Concr. Res.* 124, 105799. doi:10.1016/j.cemconres.2019.105799

Snellings, R., Suraneni, P., and Skibsted, J. (2023). Future and emerging supplementary cementitious materials. *Cem. Concr. Res.* 171, 107199. doi:10.1016/j.cemconres.2023.107199

Soudée, E., and Péra, J. (2000). Mechanism of setting reaction in magnesia-phosphate cements. *Cem. Concr. Res.* 30 (2), 315–321. doi:10.1016/s0008-8846(99)00254-9

Sugama, T., and Kukacka, L. E. (1983). Magnesium monophosphate cements derived from diammonium phosphate solutions. *Cem. Concr. Res.* 13 (3), 407–416. doi:10.1016/0008-8846(83)90041-8

Wang, D., Zhu, J., and Wang, R. (2021). Assessment of magnesium potassium phosphate cement for waste sludge solidification: macro- and micro-analysis. *J. Clean. Prod.* 294, 126365. doi:10.1016/j.jclepro.2021.126365

Xu, B., Ma, H., Shao, H., Li, Z., and Lothenbach, B. (2017). Influence of fly ash on compressive strength and micro-characteristics of magnesium potassium phosphate cement mortars. *Cem. Concr. Res.* 99, 86–94. doi:10.1016/j.cemconres.2017.05.008

Yang, Q., Zhu, B., Zhang, S., and Wu, X. (2000). Properties and applications of magnesia–phosphate cement mortar for rapid repair of concrete. *Cem. Concr. Res.* 30 (11), 1807–1813. doi:10.1016/s0008-8846(00)00419-1

Yu, B., Zhou, J., Cheng, B., and Yang, W. (2021). Compressive strength development and microstructure of magnesium phosphate cement concrete. *Constr. Build. Mater.* 283, 122585. doi:10.1016/j.conbuildmat.2021.122585

Zhang, J., Chen, J., Wan, Y. K., and Wang, L. Y. (2015). Technology of brick-making with harbor dredging silt. *Archit. Eng. NEW Mater.*

Zheng, D.-D., Ji, T., Wang, C.-Q., Sun, C.-J., Lin, X.-J., and Hossain, K. M. A. (2016). Effect of the combination of fly ash and silica fume on water resistance of Magnesium–Potassium Phosphate Cement. *Constr. Build. Mater.* 106, 415–421. doi:10.1016/j.conbuildmat.2015.12.085